

An error-sensor location Scheme in Active Vibration Isolation Based on Elastic Foundation

Wang, Chunyu¹

**Institute of Ship Noise and Vibration, Naval University of Engineering
717 Jiefang Avenue, Wuhan, Hubei, China**

Li, Yan²

**Institute of Ship Noise and Vibration, Naval University of Engineering
717 Jiefang Avenue, Wuhan, Hubei, China**

Shuai, Changgeng³

**Institute of Ship Noise and Vibration, Naval University of Engineering
717 Jiefang Avenue, Wuhan, Hubei, China**

ABSTRACT

In this paper, the problem of error-sensor location in active vibration isolation of elastic foundation under complex excitation is considered. By analyzing the vibration transmission characteristics of rigid body foundation and elastic structure foundation, this paper explains the inconsistency of attenuation effect of single-channel vibration isolation system based on rigid body supported elastically at different positions, and points out that multi-channel isolation system can solve the inconsistency problem. For elastic structure foundation, the connecting part between isolator and foundation is regarded as rigid body structure. An error-sensor location scheme of three error sensors for a single isolator is designed based on the rigid body foundation experiments. The isolation effect is achieved by controlling the vibration of three error-sensors under the isolator simultaneously. Experimental results demonstrate that the proposed scheme has the advantage of control effect and control stability compared with the traditional single error-sensor scheme.

Keywords: Active vibration control, Elastic foundation, Error-sensor location

I-INCE Classification of Subject Number:46

1.INTRODUCTION

In the field of ship vibration, underwater acoustic radiation noise caused by vibration of mechanical equipment is a major factor affecting the operation of sonar and possibility of been detected underwater. As an effective means of vibration reduction, active vibration isolation has always been a research hotspot in the field of line vibration and noise control. In order to achieve more comprehensive vibration reduction, the researchers have tried varies ways such as

¹ Wangchunyu290@163.com

² liyan19840622@yeah.net

³ chgshuai@163.com

changing the target of control, power flow^[1,2,3], elastic structure^[4,5,6] and so on, pushing the vibration isolation technology developed from single degree of freedom to multiple degrees of freedom. Corresponding multi-degree-of-freedom isolators^[7,8,9] and control algorithms have emerged, but the test equipment is complex and costly. So it has not been used in engineering application. This paper analyses the vibration attenuation inconsistency problem in the rigid and elastic foundation caused by the multi-degree-of-freedom vibration when the control force is in one-direction (always vertical) force. And an error-sensor scheme, which improves the overall vibration attenuation effect is proposed to improve the total vibration suppression.

2. PRINCIPLE OF ACTIVE VIBRATION ISOLATION SYSTEM

Active vibration isolation system is based on passive vibration isolation system, which adds vibration sensors and outputs the secondary force through the control system to cancel the original vibration transmitted to the base. The key components include control systems, actuators, and sensors. The general model of the active vibration isolation system is shown in Figure 1.

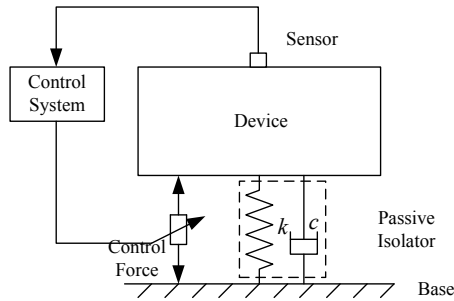


Fig. 1 The general mode of active vibration control in single freedom isolation system

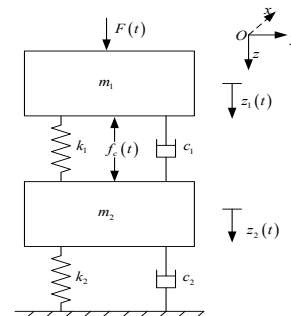


Fig. 2 The single freedom isolation system for elastic foundation

However, for the vibration isolation system in practical applications, the multi-directional excitation force, the asymmetry of the base relative excitation force and the elastic characteristics will cause the base vibration to be more than one degree of freedom, but common actuator can only produce one-direction forces. So the model in Figure 1 is no longer suitable. Figure 2 is a two-degree-of-freedom vibration isolation model, which can be regarded as a single-degree-of-freedom vibration isolation model based on the rigid-body structure supported elastically.

3. ISOLATION OF RIGID STRUCTURE FOUNDATION

3.1 Analysis of Basic Vibration Characteristics and Active Control Results of Single Isolator System

This paper analyzes problem in the two-dimensional plane for the convenience of research. Only the z-direction and the motion around the x-axis in the coordinate system of Fig. 2 are considered. It can be set that the excitation force transmitted to the foundation is $F=[f_z M_x]$, the vertical stiffness of the lower layer spring is k , and the rotational stiffness is G_x , then the basic equation of motion can be expressed as:

$$\begin{cases} f_z - kz = m_2 \ddot{z} \\ M_x - G_x \theta = I_x \ddot{\theta} \end{cases} \quad (1)$$

Where I_x is the moment of inertia of the pedestal structure along the x-axis, and θ is the angle of rotation of the base.

As described above, when the exciting force F causes the upper structure and the lower foundation to vibrate in a plurality of degrees of freedom, an actuator which can only generate a vertical force is difficult to provide a control force capable of offsetting the dynamic force transmitted to the foundation zero. For vibrations with small amplitude, the vibration of the foundation can be decomposed into a translational motion in the vertical z direction and a rotation around the x-axis according to the equation (1). When the actuator acts on the x-axis of

the foundation, the degrees of freedom do not affect each other, then the active control force can only control the vertical component transmitted to the foundation. When the actuator is not applied to the x-axis of the foundation, the vertical force generates the moment. the active control force will not only control the vertical component of the excitation force but also affect the rotation component, which is unpredictable. The rotation motion causes the phases on the left and right sides to be different, while the translation motion causes the same amplitude movement in the same phase, which inevitably leads to inconsistent vibration control effects at different positions on the base.

It may be assumed that the vertical active control force f_c acts on y_c , and the control force will provide both force and moment as f_c and M_{cx} , respectively, then equation (1) will become:

$$\begin{cases} f_z - kz - f_c = m_2 \ddot{z} \\ M_x - G_x \theta - M_{cx} = I_x \ddot{\theta} \end{cases} \quad (2)$$

And $M_{cx} = f_c * y_c$ in the equation. If the error measurement point and the control force are configured in the same position, the error acceleration signal can be expressed as:

$$a = \ddot{z} + y_c \ddot{\theta} \quad (3)$$

Let $a=0$, then simplify the equation (2) to get the optimal control force:

$$f_c = \frac{f_z(G_x - I_x \omega^2) + y_c M_x (k - m_2 \omega^2)}{(G_x - I_x \omega^2) + y_c^2 (k - m_2 \omega^2)} \quad (4)$$

Then the vibration acceleration at the measurement point y_0 on the base is

$$\begin{aligned} a_0 &= \ddot{z}_{opt} + y_0 \ddot{\theta}_{opt} \\ &= \left\{ \frac{-\omega^2 f_z}{(k - m_2 \omega^2)} \left(1 - \frac{(G_x - I_x \omega^2) + y_c M_x (k - m_2 \omega^2)}{(G_x - I_x \omega^2) + y_c^2 (k - m_2 \omega^2)} \right) \right\} \\ &\quad + y_0 \left\{ \frac{-\omega^2 M_x}{G - I_x \omega^2} \left(1 - \frac{y_c f_z (G_x - I_x \omega^2) + y_c M_x (k - m_2 \omega^2)}{(G_x - I_x \omega^2) + y_c^2 (k - m_2 \omega^2)} \right) \right\} \end{aligned} \quad (5)$$

Where \ddot{z}_{opt} and $\ddot{\theta}_{opt}$ are the optimal vertical acceleration and rotational angular acceleration. The first term is the translational vibration along the z-axis, and the second term is the rotational vibration caused by the rotation.

Set the basic mass 1000Kg, excite force frequency 60Hz, 1000N, torque 5 N*m, basic spring vertical stiffness 300N/mm, rotational stiffness 300N/rad, basic moment of inertia 500. Simulation results are shown in Figures 3 and 4.

Figure 3 shows the vibration of the measurement point ($y_0=0.1m$) with the change of the optimal control force position (point horizontal line) and the optimal control force required when the position of the control force changes (solid line). It can be seen that when the active control force is on the rotating axis, that is, $y_c=0$, the control force is equal to the exciting force, translation vibration is completely zero, while the rotation is not affected. But when $y_c \neq 0$, as the position of the control force is far away from the rotating axis, the torque generated by the control force becomes larger and larger, so the optimal control force does not increase or decrease blindly, but shows a first increase when $y_c > 0$ (optimal control force 1031N at $y_c = 0.039$) and then decreasing. When the control force position is 0.1m (that is, it is in the same position as the measurement point), the vibration of the measurement point is the smallest, and gradually increases as the position of the control force moves to both ends.

Figure 4 shows the vibrations at different base positions before and after control when the positions of the control forces are 0.07m, 0.1m, and 0.12m, respectively. It shows that the position of the control force has an important influence on the final control effect, which may cause the vibration of the measurement point to decrease or even increase.

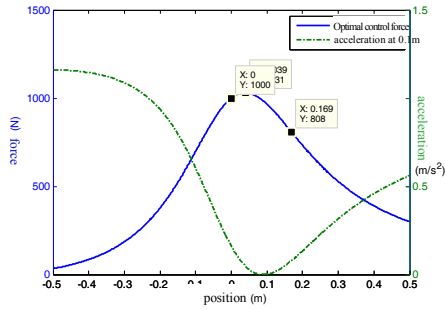


Fig. 3 The acceleration at 0.1m under the optical control force applied at different position and the needed optical control forces

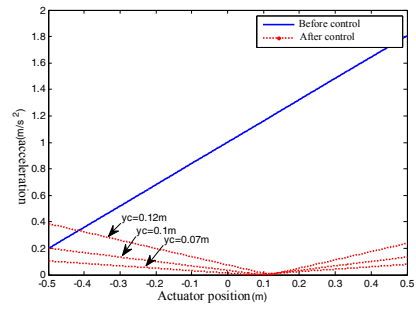


Fig. 4 The acceleration of different position when the optical control force is applied at 0.07m, 0.1m, 0.12m

Experimental verification:

In the experiment shown in Fig. 5, the foundation supported by 4 air springs, weighs about 1t, and 1m×1m×0.23m size. The first-order elastic mode frequency is 564Hz, which is far above the frequency range for controlling. An isolator (containing an actuator inside) is mounted in the middle of the foundation, and an accelerometer is installed as an error sensor at the position corresponding to the vibration isolator. 16 accelerometers are installed at the upper surface of the foundation evenly as measurement sensors to evaluate the overall vibration. An upper mass weigh about 100Kg, which is excited by the inertial actuator.

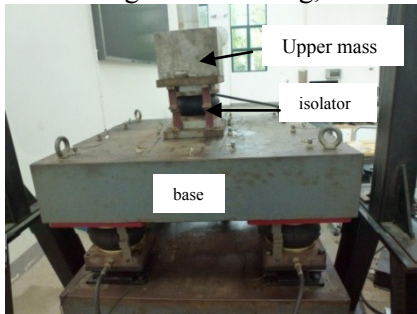


Fig. 5 The experiment device using only single isolator

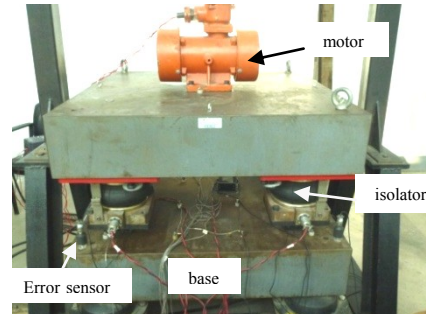


Fig. 6 The active isolation experiment device with 4 isolators

Figure 7 shows the 60s line spectral vibration energy process of the 16 sensors at 70Hz. The active control is turned on at 17s. It can be observed that the vibrations at the measurement points 1-4 are gradually decreasing. The measuring points 13-16 show the phenomenon that the vibration first decreases but then increases, which is consistent with the analysis above.

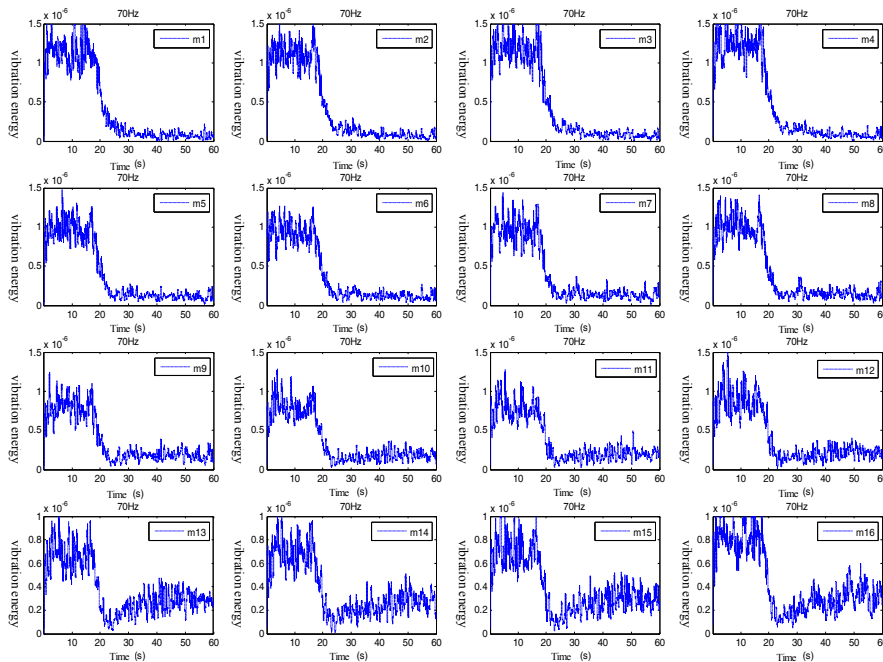


Fig. 7 The control process of 16 observe points at 70Hz

3.2 Solution - Study on Vibration Isolation Performance of Multi-isolator System

It can be seen from the above that the reason why the base cannot obtain effective vibration control is that the vertical control force cannot generate a suitable torque to suppress the rotational vibration. The torque generated by a single vibration isolator cannot match the transmitted torque, which result in the vibration of partial measurement points rebound or even diverge in the later stages of control.

Considering the vertical excitation and the rotational excitation, the vibration transmitted to the base through the isolator can be equivalent to the vibration under the action of the vertical force F and the moment M_x . If the number of vibration isolators is L , the vertical control force can be expressed as $\mathbf{F}_c=[f_{c1}, f_{c2}, \dots, f_{cL}]^T$, and the distance between each vibration isolator from the center of rotation is $\mathbf{R}=[r_1, r_2, \dots, r_L]^T$, then the problem can be expressed as solving the problem of equation (6).

$$\begin{cases} \sum_{i=0}^L f_{ci} = F \\ \mathbf{F}_c^T \mathbf{R} = M_y \end{cases} \quad (6)$$

From this it can be concluded that for basic vibrations considering only the z-axis and the x-axis. Two secondary sources are required at least to ensure complete suppression.

The test setup is as follows: 4 rubber isolators are used to support the rigid foundation, and 4 active isolators are used to connect the upper mass and foundation. Because the upper mass is heavier than the former test, the vibration motor is used as the excitation source. Four accelerometers are arranged as error sensors next to the four vibration isolators, and 16 accelerometers are evenly arranged on the base to evaluate the vibration isolation effect as same as the former test. The test device is shown in Figure 6.

Figure 8 shows the vibration process of 16 error measurement points at 60Hz. All the measurement points show consistent vibration suppression effect, and the average control effect is up to 40dB. Experiments show that the measurement point and the error measurement point can get good control effect, and there is no local measurement point increase or over-control. The vibration analysis of the rigid foundation supported elastically is verified again and the total control can be achieved in a multi-channel vibration isolation system.

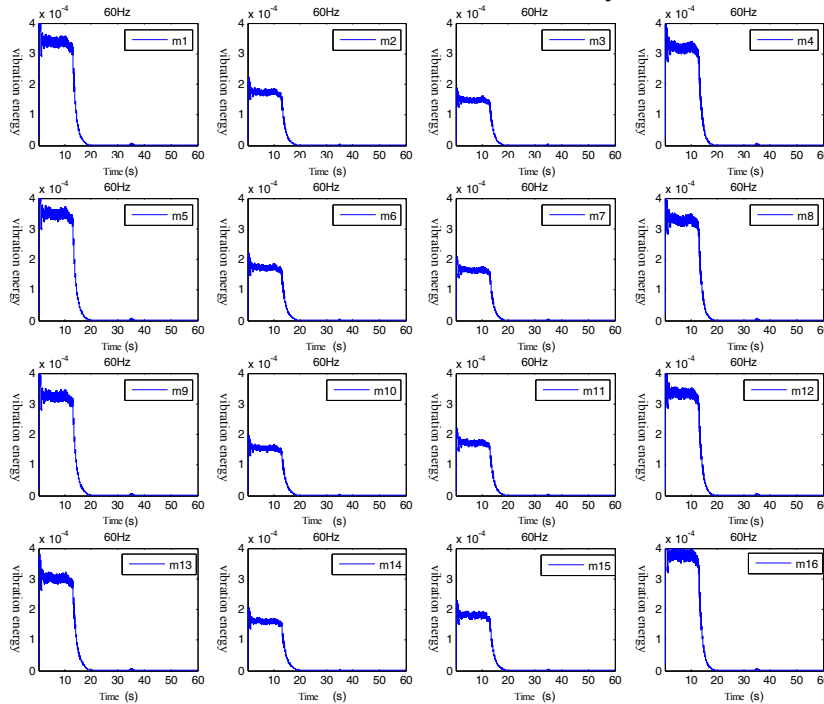


Fig. 8 The control process of each observe point at frequency 60Hz

4. RESEARCH ON VIBRATION ISOLATION OF ELASTIC STRUCTURE FOUNDATION

When the structure is excited under the condition of high frequency range or strong boundary constraint, it needs to be regarded as an elastic structure. In the mechanical vibration isolation application of ships, there are few basic structures that can be regarded as rigid bodies. The literature [9] also pointed out that in the laboratory, the foundation is often regarded as a rigid body with infinite rigidity. In fact, the impedance of the ship base is smaller than that of the test bench, which is the main reason for the deterioration of the vibration isolation effect in the application.

4.1 Vibration Characteristics of Simply Supported Beams under Complex Excitation

(1) Vibration equation of simply supported beam vibration isolation system

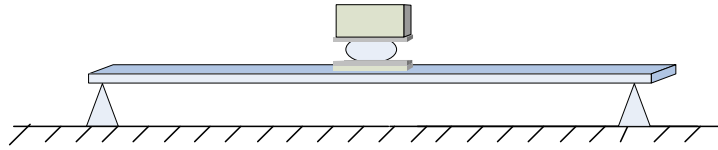


Fig. 9 The model of beam isolation system with simple supported

For the elastic vibration isolation system composed of a single vibration isolator as shown in Fig. 9, the power transmitted to the foundation by the literature [10] is

$$Power = \frac{\omega}{2} \text{Im}\{[\mathbf{D}^b]^H (\mathbf{Q}^b + \mathbf{Q}_c)\} = \frac{\omega}{2} \text{Im}\{[F_c^T a F_c + F_c^T b_1 + b_2 F_c + c]\} \quad (7)$$

which

$$\begin{aligned} a &= [[\mathbf{G}_1]K[\mathbf{G}_2] - [\mathbf{G}_1]] & b_1 &= [\mathbf{G}_1]K[\mathbf{G}_3] \\ b_2 &= [\mathbf{G}_4]K[-\mathbf{G}_2] + \mathbf{G}_4 & c &= \mathbf{G}_4 K[-\mathbf{G}_3] \end{aligned} \quad (8)$$

\mathbf{Q}^b and \mathbf{Q}_c are the primary and active control forces of the vibration isolator to the underlying foundation respectively. When $\mathbf{Q}_c=0$, it is equivalent to the passive vibration isolation system. Equation (7) is the total vibration energy transmitted by the initial excitation in the simply supported beam vibration isolation system.

(2) Characteristics of vibration transmitted to the beam under different excitations

In order to visualize the energy law that the excitation source is transmitted to the foundation, the numerical simulation of the equation (7) is carried out. The specific simulation parameter settings are shown in Table 1.

Tab. 1 The simulation setup in beam isolation system with simple supported

the upper mass 7.88Kg	Beam moment of inertia $I=1.25 \times 10^{-8} \text{ m}^4$
Size of the upper mass 0.1m×0.15m×0.14m	Location of isolator 0.76m
The lower mass 7.44Kg	Modal loss factor of beam 0.0047
Size of beam: 1.52m length, 0.0015m ² Cross-sectional area	Vertical stiffness of the isolator 31250 N/m
Beam density 2770Kg/m ³	Rotational stiffness of the isolator 316 N·m/rad
Elastic modulus of the beam $E=6.895 \times 10^{10} \text{ N/m}^2$	

The vertical excitation force $F_z=1\text{N}$, the hybrid excitation force $F_z=1\text{N}$ and $M_y=0.01\text{N}\cdot\text{m}$, and the hybrid excitation force $F_z=1\text{N}$ and $M_y=0.02\text{N}\cdot\text{m}$ are respectively set. Figure 10 shows the variation of the vibration energy transmitted to the foundation with the excitation frequency for three excitations. Under the excitation of $F_z=1\text{N}$ and $M_y=0.01\text{N}\cdot\text{m}$, the energy transmitted to the foundation is shown in Figure 11 when stiffness of the isolator changes.

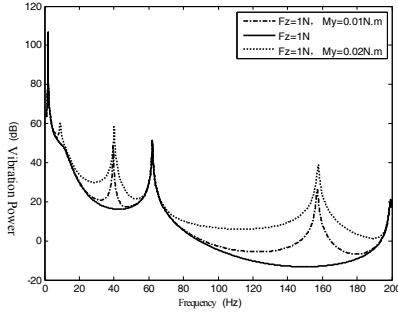


Fig. 10 The comparison of power transmitted when three kinds of excited forces

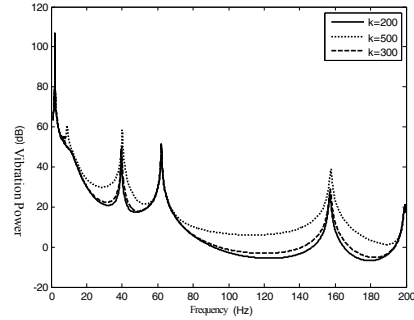


Fig. 11 The comparison of power transmitted with different isolator rotational stiffness

The simulation results show that at the resonance frequency point of the beam, the vibration of the pedestal is enhanced and the transmitted energy is increased, which is consistent with the transmission characteristics of the single-layer vibration isolation system. However, in the case of complex excitation, a resonance frequency is added to the resonance point within 200 Hz, which is the resonance frequency of the upper mass and the isolator in the direction of rotation. At this frequency, the rotational energy is greatly enhanced, much higher than vertical. It can also be seen in Fig. 10 that the contribution of the moment excitation to the vibration of the pedestal is not very obvious in the low frequency band, and gradually increases with the increase of the frequency, which is consistent with the analysis in the literature [11]. The greater the torque excitation, the greater the impact on the foundation. When changing the rotational stiffness of the isolator, the greater the stiffness, the greater the energy delivered to the foundation, and this feature is also more pronounced in the high frequency band. This phenomenon is a positive signal for the active control of the low frequency line spectrum.

The above analysis shows that the vibration energy components transmitted to the elastic foundation include vertical excitation and rotational excitation, and it is necessary to have both vertical control force and rotational control force to control the vibration transmitted by the excitation force.

4.2 Solution - Optimization error sensor arrangement

In general, the position of the sensor in the active vibration isolation system only needs to be able to detect the vibration signal effectively. and it is usually placed in the same position as the vibration isolator. However, it is undeniable that there is a phenomenon of poor vibration isolation at individual local locations. So the vibration of the whole structure cannot be guaranteed. Therefore, the sensor's position optimization must have certain guiding principles to achieve better control results.

In the rigid body structure, the torque can be equivalent to two point forces acting at different positions. Considering that the air spring isolator has a certain contact area when connecting the upper machine and the lower foundation, and the thickness is often increased at the installation position to strengthen the structural strength. Therefore, in this paper, the base part of the lower cover of the vibration isolator (actuator) is regarded as a local rigid body, and the excitation force transmitted through the vibration isolator and control force are equivalent to the surface force acting on the lower cover. When both can be completely offset, the vibration energy can be considered to be effectively attenuated. Combined with the above research on active vibration isolation of rigid structures, it can be judged that when the initial excitation source contains complex components such as rotation, if only relying on the vibration at one measuring point position as the target of vibration control, the control effect and the sensor location is closely related. According to the decomposition of the vibration, when the error sensor is located in the middle position of the panel, the control of the vibration of the error measuring point represents that the energy of the vertical translation is effectively controlled, and the rotational energy is not affected; when the error sensor is located at the side of the middle of the panel The vibration of other measuring points at the panel may increase, and the overall control effect is worse.

Based on the condition that the actuator only produces the vertical control force, this paper proposes an arrangement scheme in which multiple sensors correspond to one vibration

isolator, and the vibration signal measured by multiple error sensors is used as the test and control for transmitting vibration of a single vibration isolator, so as to achieve the purpose of improving the control effect of the other measuring points. By comparing the vibration isolation effects of different error sensor arrangements, the final solution of the error point arrangement is determined.

The traditional sensor arrangement uses an error measuring point corresponding to a vibration isolator. Two comparison schemes are set separately: the sensor is located at the center and eccentric of the installation part of the lower cover of the vibration isolator. In addition, according to the principle that one plane can be determined by three points, Three accelerometers are arranged on the lower surface of the isolator in equilateral triangle as error sensors. If the acceleration at these three positions are effectively suppressed, it can be judged that the vibration is completely isolated on the transmission path. The three arrangements for participating in the test comparison are shown in Figure 12.

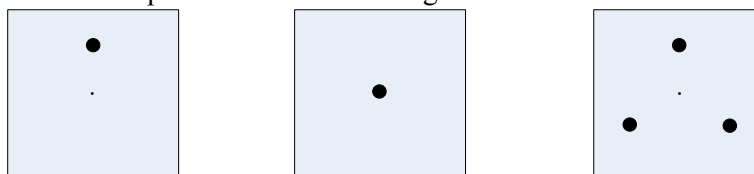


Fig. 12 The three error sensor location schemes

4.3 Experimental Research - Comparison of Error Pointing Schemes

A single vibration isolator test platform based on simply supported beams was constructed. The dimensions of the beams are 1500mm×180mm×25mm. The two ends are supported by a wedge-shaped structure, the position of the vibration isolator is in the middle of the structure, the upper mass is about 20Kg, the size is 200mm×200mm×100mm, and the vibration source is a hanging inertial vibration exciter. In order to evaluate the vibration isolation effect more objectively, 18 BK accelerometers (6 rows and 3 columns) are evenly arranged on the upper surface of the simply supported beam, and the average value of the acceleration signals collected by these accelerometers is used as an evaluation index of the vibration isolation effect.

According to the position of the primary excitation point, two sets of experimental conditions (see Fig. 13) are set to simulate the complex excitation vibration source, and three error sensor arrangement schemes are compared and tested respectively, as shown in Table 2. In the test, the frequency of the excitation signal is from 35 Hz to 100 Hz, and the frequency interval is 5 Hz. The control process data from the pre-control is recorded and analyzed. The real scene of the three schemes is shown in Fig. 14, and a total of four acceleration error sensors are required.

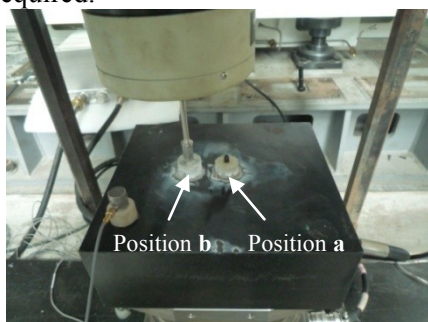


Fig. 13 The exciter positions of two work conditions



Fig. 14 The picture of three error sensor location strategies

Tab. 2 The exciter experiment setup

Excitation conditions	Error sensor arrangement
Case a: The exciter excitation point is at position a	Eccentric single error measuring point (Scheme 1)
	Center single error measurement point (Scheme 2)

Central symmetric three measuring points (Scheme 3)

Eccentric single error measuring point (Scheme 1)

Case b: The exciter excitation point is at position b

Center single error measurement point (Scheme 2)

Central symmetric three measuring points (Scheme 3)

Before the test, the vibration characteristics at the installation position of the isolator on the foundation under the excitation of the primary source (exciter) and the secondary source (actuator) were first tested using four error sensors. Figure 15 shows the phase consistency of four error sensors for case a. It can be seen that although the amplitudes at the four positions are different but the phases are relatively consistent below 70 Hz, which prove that the vertical translation is the main form of vibration. However, the phase difference above 70 Hz gradually increases, indicating that the proportion of rotational motion is gradually increasing. Figure 16 shows the phase consistency in case b. It can be seen that the eccentric excitation causes the rotational energy to increase at 60 Hz.

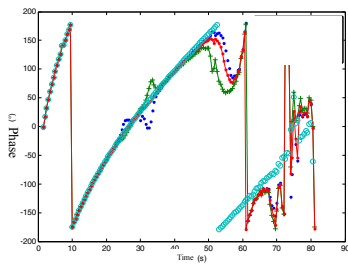


Fig. 15 The phase relationship of vibration signals at 4 points under isolator excited by exciter

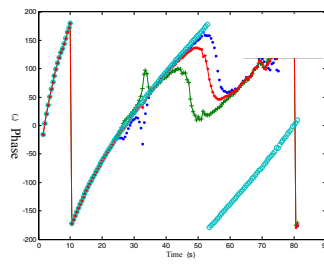


Fig. 16 The phase relationship of vibration signals at 4 points under isolator excited by actuator

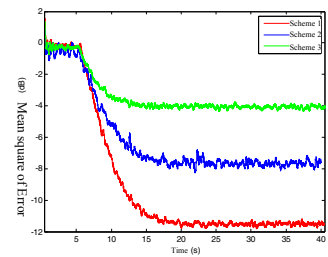


Fig. 17 The comparison of convergence of error measuring points at 70 Hz

Figure 17 shows the (average) convergence process (MSE, mean square of error) of the error measurement points of the three schemes at 70 Hz in case b. It can be seen that in the single error layout scheme (Scheme 1 and Scheme 2), the error measurement points can get a good convergence effect, and the vibration line spectrum can almost converge to the background noise level (This also confirms the correctness of the control algorithm and is independent of the position of the error measurement point). While the vibration suppression of the error measurement point in the scheme 3 is worse than the former two schemes. But this is normal for the over-determined system.

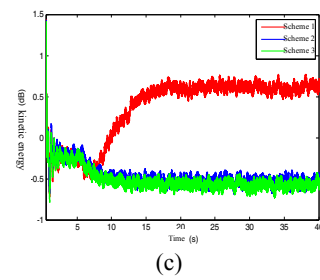
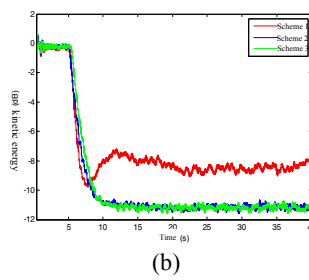
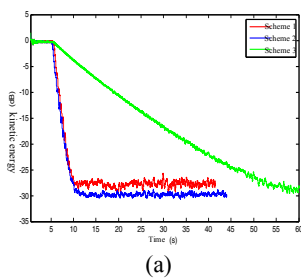


Fig. 18 The average convergence process of 18 observe points in three arrangement at 35Hz(a)、50Hz(b)、70Hz(c)

Figure 18 is a comparison of the kinetic energy (calculated from 18 measurement points) at the frequencies of 35 Hz, 50 Hz, and 70 Hz after the implementation of the three schemes in case b. It can be seen that at the low frequency (30 Hz), those three schemes have small differences and the convergence effect is equivalent. And in the high frequency (50Hz and 70Hz) schemes 2 and 3 still have similar convergence characteristics. But in the scheme 1, the vibration suppression effect first increases and then decreases, which is because the vibration measured by the current error measurement points contains the components caused by rotational excitation. When the vibration is in the low frequency range, the rotational component is relatively small. As the frequency increases, the rotational component increases, so the control algorithm would increase the control force to reduce the vibration of the error point, resulting in

excessive control and the overall vibration is increased finally. The greater the rotational component, the more pronounced this phenomenon (the vibration is more strongly rebounded at 70 Hz than at 50 Hz in Scheme 1.).

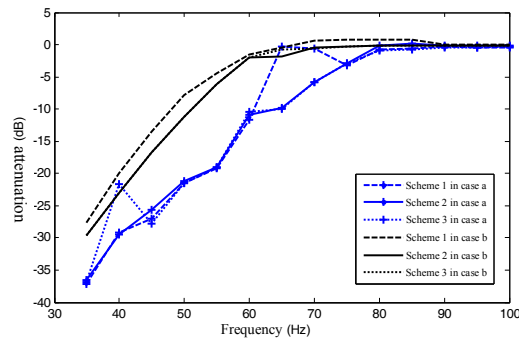


Fig. 19 The average attenuation of 18 observe points in three arrangement at each work condition

Figure 19 shows the average vibration suppression of the three schemes at each frequency under two cases. It can be seen that the average control effect of the three schemes in case a is close except for individual frequencies, but the difference between the schemes in case b is large. In the same scheme, case b is worse than case a, because the exciting position b is more eccentric than position a, that is, the primary exciting rotational component is larger in case b. In the low frequency band (below 70 Hz), the vibration has obvious suppression after active control. However, in the high frequency range, the suppression is gradually reduced as the frequency increases due to the individual points are diverged in all schemes. There is almost no suppression at above 90 Hz. This is because it is actually difficult to guarantee the position excited is exactly in the center of the upper mass so the actuator cannot match the force transmitted from the upper mass.

In addition, carefully compare the vibration isolation effect of scheme 2 and scheme 3, it can be seen the suppression of scheme 3 is slightly better than scheme 2, and the vibration of the whole structure can be more reflected in scheme 3. Moreover, in practical applications, the error sensor is difficult to be centered due to reasons such as reinforcing ribs. If there is too much deviation from the center, the overall suppression effect will be poor or even divergence. Considering that, Scheme 3 is more operative.

5. CONCLUSIONS

In this paper, the rigid body structure and the elastic structure foundation transfer characteristics of the elastic support in the active vibration isolation system are analyzed. The multi-isolator system is used to solve the global vibration control problem of the rigid body foundation vibration. For the elastic structure foundation, an error sensor arrangement scheme with three error sensors corresponding to one vibration isolator is designed. The experimental results compared with the former location of the error sensors show that the arrangement of three error sensors with one actuator can ensure that the isolation system obtains more vibration information about the base and improves the overall vibration isolation effect.

6. REFERENCES

- [1] GOYDER H G D, WHITE R G. "Vibration power flow from machines into built-up structures. Part I : Introduction and approximate analyses of beam and plate-like foundations". Journal of sound and vibration, 1980, 68(1): 59-75.
- [2] GOYDER H G D, WHITE R G. "Vibration power flow from machines into built-up structures. Part II : Wave propagation and power flow in beam-stiffened plates". Journal of sound and vibration, 1980, 68(1): 77-96.
- [3] GOYDER H G D, WHITE R G. "Vibration power flow from machines into built-up structures. Part III: Power flow through isolation systems". Journal of sound and vibration, 1980, 68(1): 97-117.

- [4] Jie Pan, Jiaqiang Pan. “*Total power flow from a vibrating rigid body to a thin panel through multiple elastic mountsnoise*”. The Journal of the Acoustical Society of America, 1992.
- [5] Jiaqiang Pan, Colin H. Hansen. “*Active control of power flow from a vibrating rigid body to a flexible panel through two active isolators*”. The Journal of the Acoustical Society of America, 1993.
- [6] Jiaqiang Pan, Colin H. Hansen. “*Active isolation of a vibration source from a thin beam using a single active mount*”. The Journal of the Acoustical Society of America, 1993.
- [7] Ross, C. F., Scott, J. F., Sutcliffe, S. G. C. “*Active control of vibration*”, International Patent Application, 1988, No. PCT/GB87/00902.
- [8] Ross, C. F., Scott, J. F., Sutcliffe, S. G. C., “*Active control of vibration*”, 1989, US Patent No. 5,433,422.
- [9] Wei Qiang, Zhu Yingfu, Zhang Guoliang. “*Numerical Analysis of Single-layer Vibration-isolating System on Shipboard Base*”. SHIP ENGINEERING, 2004, 26(3): 37-40.
- [10] Carl Howard. “*Active isolation of Machinery vibration from flexible structure*”, University of Adelaide, 1999.
- [11] GARDONIO P, S J E. “*Active isolation of structural vibration on a multiple degree of freedom system, part I_ the dyna*”. Journal of Sound and Vibration, 1997. 207(1): 61-93.